

## Maximum Power Point Tracking Charge Controller for Standalone PV System

Mohd Asri Jusoh<sup>1</sup>, Mohammad Faridun Naim Tajuddin<sup>\*2</sup>, Shahrin Md Ayob<sup>3</sup>,  
Mohd Azrik Roslan<sup>4</sup>

<sup>1,2,4</sup>School of Electrical Systems Engineering, Universiti Malaysia Perlis (UniMAP), Malaysia

<sup>3</sup>Faculty of Electrical Engineering, Universiti Teknologi Malaysia, Malaysia

\*Corresponding author, e-mail: asrijusoh@unimap.edu.my<sup>1</sup>, faridun@unimap.edu.my<sup>2</sup>,  
shahrin@fke.utm.my<sup>3</sup>, mazrik@unimap.edu.my<sup>4</sup>

### Abstract

The depletion of conventional energy sources and global warming has raised worldwide awareness on the usage of renewable energy sources particularly solar photovoltaic (PV). Renewable energy sources are non-polluting sources which can meet energy demands without causing any environmental issues. For standalone PV systems, a low conversion efficiency of the solar panel and high installation cost due to storage elements are the two primary constraints that limit the wide spread use of this system. As the size of the system increases, the demand for a highly efficient tracking and charging system is very crucial. Direct charging of battery with PV module will result in loss of capacity or premature battery degradation. Furthermore, most of the available energy generated by the PV module or array will be wasted if proper tracking technique is not employed. As a result, more PV panels need to be installed to provide the same output power capacity. This paper presents selection, design and simulation of maximum power point tracker (MPPT) and battery charge controller for standalone Photovoltaic (PV) system. Contributions are made in several aspects of the whole system, including selection of suitable converter, converter design, system simulation, and MPPT algorithm. The proposed system utilizes direct duty cycle technique thus simplifying its control structure. MPPT algorithm based on scanning approach has been applied by sweeping the duty cycle throughout the I-V curve to ensure continuous tracking of the maximum power irrespective of any environmental circumstances. For energy storage, lead acid battery is employed in this work. MATLAB/Simulink® was utilized for simulation studies. Results show that the propose strategy can track the MPPs and charge the battery effectively.

**Keywords:** SEPIC converter; maximum power point tracking (MPPT); charge controller; standalone photovoltaic (PV) systems

Copyright © 2018 Universitas Ahmad Dahlan. All rights reserved.

### 1. Introduction

Among the alternative energy sources, solar energy is one of the most widely used and readily available renewable energy sources. Solar energy supplied by the sun in one hour is equal to the energy required by the human population in a year. Power generated by PV module depends upon the solar irradiation, cell temperature and load impedance [1–4]. To efficiently utilize solar energy, maximum power point tracking (MPPT) technology is normally employed to ensure continuous operation of the PV systems at its maximum power point. Various MPPT strategies were utilized in the literature to adjust the maximum output power of the PV systems with the change in solar irradiance and temperature. In general, there is only one maximum power point on the P-V curve of a PV module where it produces maximum output power under uniform solar irradiance condition. Thus, in order to achieve maximum efficiency for PV systems, some conventional maximum power point tracking algorithms such as Hill-Climbing, Perturb&Observe (P&O), Incremental Conductance (Inc. Cond) [5] were employed.

In order to maximize the power transfer from the photovoltaic array to the battery bank, a battery charger with charge controller should be utilized. It performs two main functions. The first one is to accurately track the maximum power point (MPP) regardless of how quickly atmospheric conditions change. The other function is to minimize the battery charging time to back up the PV arrays as fast as possible while ensuring its safety and life cycle [6]. The battery charging control methods can be classified into two classes: (i) single stage, and (ii) multi-stage method. The constant current charging is a good example for single stage method, while

constant voltage technique is a good example for multistage charging method. Studies show that, the multi-stage charging is the most efficient for battery charging regardless of the battery type [7].

The algorithm of a battery charge controller determines the effectiveness of battery charging as well as the PV array utilization, and ultimately the ability of the system to meet the electrical load demands. The most common approaches for charge controllers are the shunt, series, pulse width modulation (PWM) and MPPT charge controllers. The shunt regulator controls the charging of a battery from the PV array by short-circuiting the array internal to the controller. The series controller utilizes some type of control element connected in series between the array and the battery. While this type of controller is commonly used in small PV systems, it is also a practical choice for larger systems due to the current limitations of shunt controllers. The MPPT battery charge controller incorporates a DC-DC converter such that the PV array can operate at the maximum power point at the prevailing solar irradiance. The structure of battery charge controllers depends on the type of the controller. In the series and shunt controllers, it simply consists of a switching element, such as a relay that is switched on/off based on the value of a predefined set point. In a PWM and MPPT controllers, the circuits are more sophisticated. In PWM generator circuits, microcontrollers are needed in order to drive the switches of a DC-DC converter while MPPT controller consists of a controller that manages the maximum power point tracking process and DC-DC converter [8]. In this paper, a DC-DC SEPIC converter is selected and has been employed for standalone PV system application. Using this converter, the PV system is able to execute good MPPT and charging control performance.

This paper is organized in the following manner: Section 2 is the research method which provides a review of standalone photovoltaic charging, with an emphasis on various battery charging control and MPPT methods. In order to validate the suggested system, simulation results together with discussions are provided in Section 3. The operation of the proposed solar charger, including the transitions between the MPPT and CV modes, are explained in this section. Lastly, conclusion is presented in Section 4.

## 2. Research Method

### 2.1. Standalone Photovoltaic (PV) Charging Systems

Solar energy systems can generally be categorized into i) standalone PV systems which consist of a PV panel, battery and load; and ii) grid connected PV systems which feed additional power to the grid. Standalone PV systems are essential as they provide a power solution for remote and isolated areas which are unreachable by grid [9]. Red dotted line in Figure 1 shows the typical components of a standalone PV charging system.

Batteries are the power tank of solar power systems. They play the role of power supply when the sun does not shine. Batteries can be avoided from reaching either overcharged or over discharged condition by implementing a charge controller into the system. Furthermore, inverter is used to convert dc to ac if there is alternating current load being used.

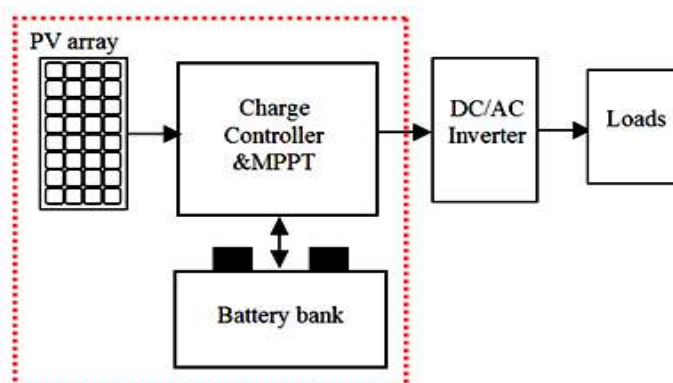


Figure 1. Typical components of standalone PV charging system

## 2.2. PV Array

A photovoltaic module consists of a number of interconnected solar cells and they can be arranged in series or parallel configurations to maximize the power for high-power applications. Solar cells consist of a  $p$ - $n$  junction fabricated in a thin layer of semiconductor [10]. A solar cell equivalent electrical circuit can be represented by a single-diode model as shown in Figure 2. Generally, the maximum output power produced depends on the applications used ranging from hundred watts to kilowatt or even megawatt. Figure 3 shows the equivalent circuit of the PV module arranged in NP parallel and NS series. Array can be formed when more modules are wired together. More electricity can be produced by using a larger area of module or array. Five different array configurations are reported in this paper. These are series (S), series-parallel (SP), total-cross-tied (TCT), bridged-link (BL), and honey-comb (HC) [11]. The relationship between the cell terminal current and voltage is as follows: [12-14]:

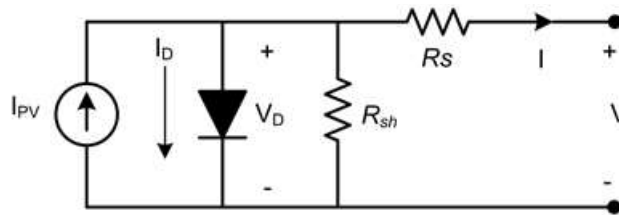


Figure 2. Equivalent circuit of PV cell

$$I = I_{pv} - I_o \left[ \exp \left( \frac{V + I \times R_s}{a \times V_{th}} \right) - 1 \right] - \frac{V + I \times R_s}{R_{sh}} \quad (1)$$

where  $I$  and  $V$  are the output current and output voltage of the photovoltaic cell, respectively.  $I_o$  is the diode's reverse saturation current,  $a$  is the diode ideality factor,  $R_s$  and  $R_{sh}$  is the series and parallel resistance, respectively.  $V_{th}$  is the thermal voltage of the cell, which is expressed as,

$$V_{th} = \frac{K_b \times T}{q} \quad (2)$$

where  $q$  is the electron charge ( $1.602 \times 10^{-19}$  C),  $T$  is the junction temperature in Kelvin (K), and  $K_b$  is the Boltzmann constant ( $1.380 \times 10^{-23}$  J/K).  $I_{pv}$  is the generated photocurrent; it depends mainly on the radiation and cell's temperature, which is expressed as,

$$I_{pv} = [I_{sc\_STC} + K_i(T - T_{STC})] \frac{G}{G_{STC}} \quad (3)$$

where  $I_{sc\_STC}$  (in Ampere, A) is the short-circuit current at standard test conditions (STC),  $T_{STC}$  ( $25^\circ\text{C}$ ) is the cell temperature at STC,  $G$  (in watts per square meters,  $\text{W}/\text{m}^2$ ) is the irradiation on the cell surface,  $G_{STC}$  ( $1000 \text{ W}/\text{m}^2$ ) is the irradiation at STC, and  $K_i$  is the short circuit current coefficient, usually provided by the  $V_{oc\_STC} + K_v(T - T_{STC})$  cell manufacturer. In addition, the saturation current  $I_o$  is influenced by the temperature according to the following equation [14-15]

$$I_o = \frac{I_{sc\_STC} + K_i(T - T_{STC})}{\exp \left[ \frac{V_{oc\_STC} + K_v(T - T_{STC})}{a \times V_{th}} \right] - 1} \quad (4)$$

where  $V_{oc\_STC}$  (in Volt, V) is the open circuit voltage at STC;  $K_v$  is the open circuit voltage coefficient, these values are available on the datasheet provided by module's manufacturer.

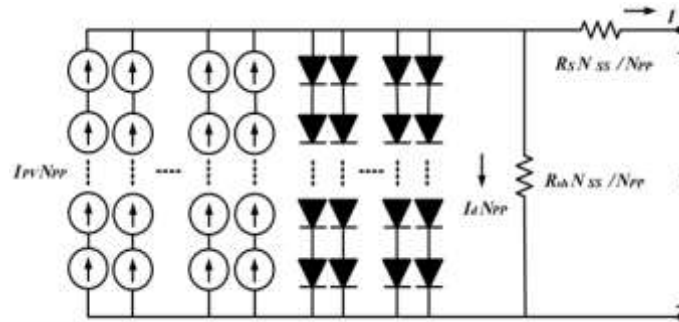


Figure 3. Equivalent circuit of PV module

The equation for PV array can be expressed as (5). The specifications for the PV module used in this paper are given in Table 1. Using these parameters, the model of the PV module is developed in MATLAB/ Simulink®, and the corresponding *I-V* and *P-V* curves under varying irradiances and at 25°C temperatures are plotted in Figure 4.

$$\begin{aligned}
 V_A &= N_{SS} \times V_{mod} \\
 I_A &= N_{PP} \times I_{mod} \\
 V_{OCA} &= N_{SS} \times V_{OCmod} \\
 I_{SCA} &= N_{PP} \times I_{SCmod} \\
 R_{SA} &= \frac{N_{SS}}{N_{PP}} R_{Smod}
 \end{aligned}
 \tag{5}$$

Table 1. Specification of PV module at STC (1000W/25°C)

Parameters	Variable	Value	Unit
Power	$P_{PV}$	10	W
Open circuit voltage	$V_{OC}$	4.48	V
Short circuit current	$I_{SC}$	2.96	A
Voltage at maximum power	$V_{MPP}$	3.66	V
Current at maximum power	$I_{MPP}$	2.74	A
Temperature coefficient of $V_{OC}$	$T_{VOC}$	-0.32	%/°C
Temperature coefficient of $I_{SC}$	$T_{ISC}$	0.09	%/°C
Number of cell	$N_{CELL}$	12	-

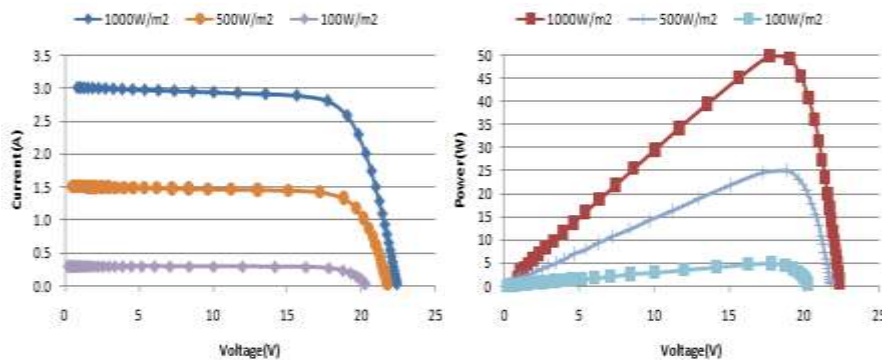


Figure 4. (a) *I-V* (b) *P-V* characteristics of PV module

### 2.3. MPPT Charge Controller

The ultimate goal of a charge controller in standalone PV systems is to maintain the highest possible state of charge while preventing battery overcharge during high solar insolation

and avoid over discharging during low insolation and excessive loading. A good charge controller does this with the least amount of PV energy being dumped. Charge controllers can be classified as on/off controllers and soft controllers [16]. Using an MPPT algorithm is a good choice in these situations, because working parameters are continuously adjusted in order to reach the optimal energy extraction [12].

**2.3.1. DC-DC Converter Selection**

When proposing an MPP tracker, the major task is to choose and design a highly efficient converter, which supposed to be operated as the main part of the MPPT charge controller. The efficiency of switch-mode DC-DC converters is widely discussed in [17]. Most switching-mode power supplies are well designed to function with high efficiency. Among all DC-DC converter topologies, buck–boost, Cuk and SEPIC converters provide the opportunity to have either higher or lower output voltage compared with the input voltage. Although the buck–boost configuration is cheaper due to its less components count compared to than Cuk and SEPIC converters, it has some disadvantages that makes it less efficient such as discontinuous input current, high peak currents in power components, and poor transient response. On the other hand, the SEPIC converter has low switching losses and the highest efficiency among non-isolated DC-DC converters. It can also provide a better output current characteristic due to the inductor on the output stage. Thus, the SEPIC configuration is a proper converter to be selected as the MPPT charge controller.

Figure 5 shows a DC-DC SEPIC converter (battery charge controller) with MPPT control. The SEPIC converter has two modes of operation. The first mode of operation is when the switch is closed (ON). In this mode, the capacitor releases energy to the output. Second operating mode is when the switch is open (OFF), in which the diode is in forward-biased and the energy is supplied to the load/battery. Capacitor C1 is charging from the PV supply. Figure 6 shows SEPIC converter in both operating modes, which is used as the intermediate stage between the PV module and the battery.

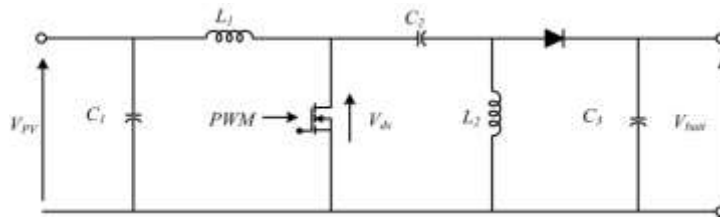


Figure 5. SEPIC converter based battery charge controller

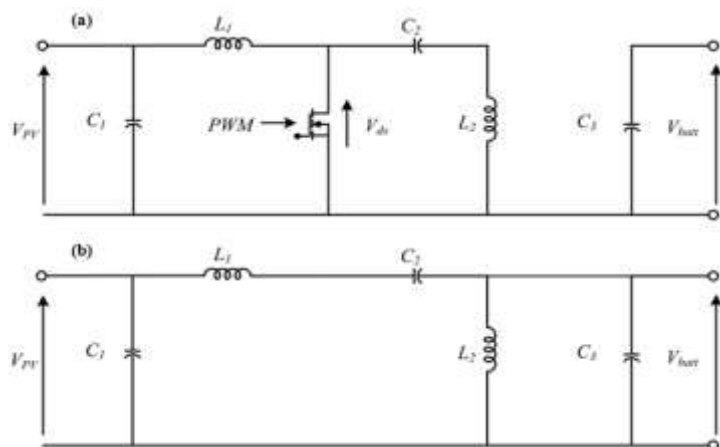


Figure 6. SEPIC converter with (a) switch ON [DT] (b) switch OFF [(1-D) T]

Where

D: Duty cycle of PWM signal (%)

T: Period PWM signal (s)

From 0 to DT: the switch is closed and diode is open, so current across  $L_1$  increase at the rate of:

$$\frac{di_{L1}}{dt} = \frac{V_{PV}}{L_1}, \quad 0 \leq t \leq Dt \quad (6)$$

So that  $L_1$  and  $L_2$  are charging;  $C_2$  and  $C_3$  are discharging. From DT to T: the switch is open and diode is closed, so current across  $i_{L1}$  decrease at the rate of:

$$\frac{di_{L1}}{dt} = \frac{-V_{batt}}{L_1}, \quad DT \leq t \leq T \quad (7)$$

So that  $L_1$  and  $L_2$  are discharging;  $C_2$  and  $C_3$  are charging.  $V_{L1}$  has two levels, their average equals zero:

$$\frac{(V_{PV})DT + (-V_{batt})(1-D)T}{T} = 0 \quad (8)$$

So that:

$$(V_{PV})D + (-V_{batt})(1-D)T = 0 \quad (9)$$

Simplifying above equation, the final input-output voltage expression:

$$V_{batt} = V_{PV} \times \frac{D}{1-D} \quad (10)$$

Thus, the converter performs buck function mode for D less than 0.5, and boost function mode for D larger than 0.5. The ripple current across both inductors,  $L_1$  and  $L_2$  is given approximately by:

$$\Delta I_L = 40\% \times I_{PV(max)} \quad (11)$$

The values of  $L_1$  and  $L_2$ :

$$L_{1(min)} = L_{2(min)} = \frac{V_{PV(min)} \times D}{2 \times \Delta I_L \times f} \quad (12)$$

The selection of capacitor  $C_2$  and  $C_3$  are given:

$$C_{2(min)} = \frac{I_{batt} \times D}{\Delta V_{ripple} \times f} \quad \& \quad C_{3(min)} = \frac{I_{batt} \times D}{\Delta V_{ripple} \times f} \quad (13)$$

$$\Delta V_{ripple} = 1\% \times V_{batt} \quad (14)$$

The relations between input and output of a SEPIC converter are given in the following:

$$\begin{aligned} P_s &= P_o \\ V_s I_s &= V_o I_o \\ V_s &= V_{PV} = V_{L1} = V_{C2} \\ V_o &= V_{batt} \\ I_s &= I_{L1} \\ I_o &= I_{L2} \end{aligned} \quad (15)$$

$$D = \frac{V_o}{V_s + V_o} \Delta V_o / V_o \quad (16)$$

The specifications of the designed converter are listed in Table 2.

Table 2. SEPIC converter design parameters

Parameter	Value
Output power, $P_o$	50 W
Maximum input voltage, $V_i$	30 V
Maximum input current, $I_i$	3.5 A
Switching frequency, $f_s$	200 kHz
Maximum inductor current ripple, $\Delta i_{O,max}$	$\leq 30\%$
Output voltage ripple, $\Delta V_o / V_o$	$\leq 3\%$
Inductor, $L_1$ and $L_2$	100 $\mu$ H
Input capacitor, $C_1$	820 $\mu$ F
Capacitor, $C_2$	660 $\mu$ F
Capacitor, $C_3$	660 $\mu$ F

### 2.3.2. Battery Charging Method

On the other hand, the controller uses a multi-stage charging algorithm, which is the most safe and effective method of charging [6]. The principle of battery charging is shown in Figure 7. In the first stage, the battery voltage is increased gradually to the preset voltage level, which is called the bulk level using constant charge current. When the bulk level voltage is reached, the absorption stage starts. During this phase, the voltage is maintained at a bulk voltage level for specific time while the current is gradually dropping. After the absorption time passes, the float stage begins. The voltage is lowered to the float level and the battery draws a very small current [6].

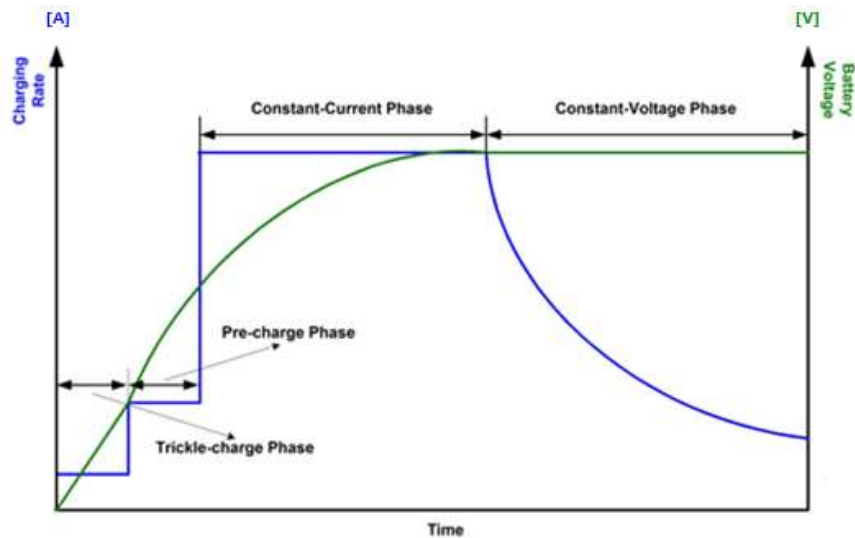


Figure 7. Battery charging characteristics

### 2.3.3. MPPT Techniques

MPPT methods can be roughly classified into two categories: there are conventional methods, like the Perturbation and Observation (P&O) [18–20], the Incremental Conductance (Inc.Cond) [21–24] and hill climbing and advanced methods (soft computing), such as fuzzy logic control [25–27], artificial neural network and particle swarm optimization have the ability to differentiate between the global MPP and local MPPs for non-uniform irradiance conditions.

In this paper, duty cycle sweeping technique is selected as the fundamental algorithm. This method is a very effective when the entire PV array is under the uniform solar irradiance condition. Herein, duty cycle control has been chosen and adjusted directly in the algorithm [28]. Figure 8 shows the flowchart of the MPPT algorithm for SEPIC converter based solar charge controller.

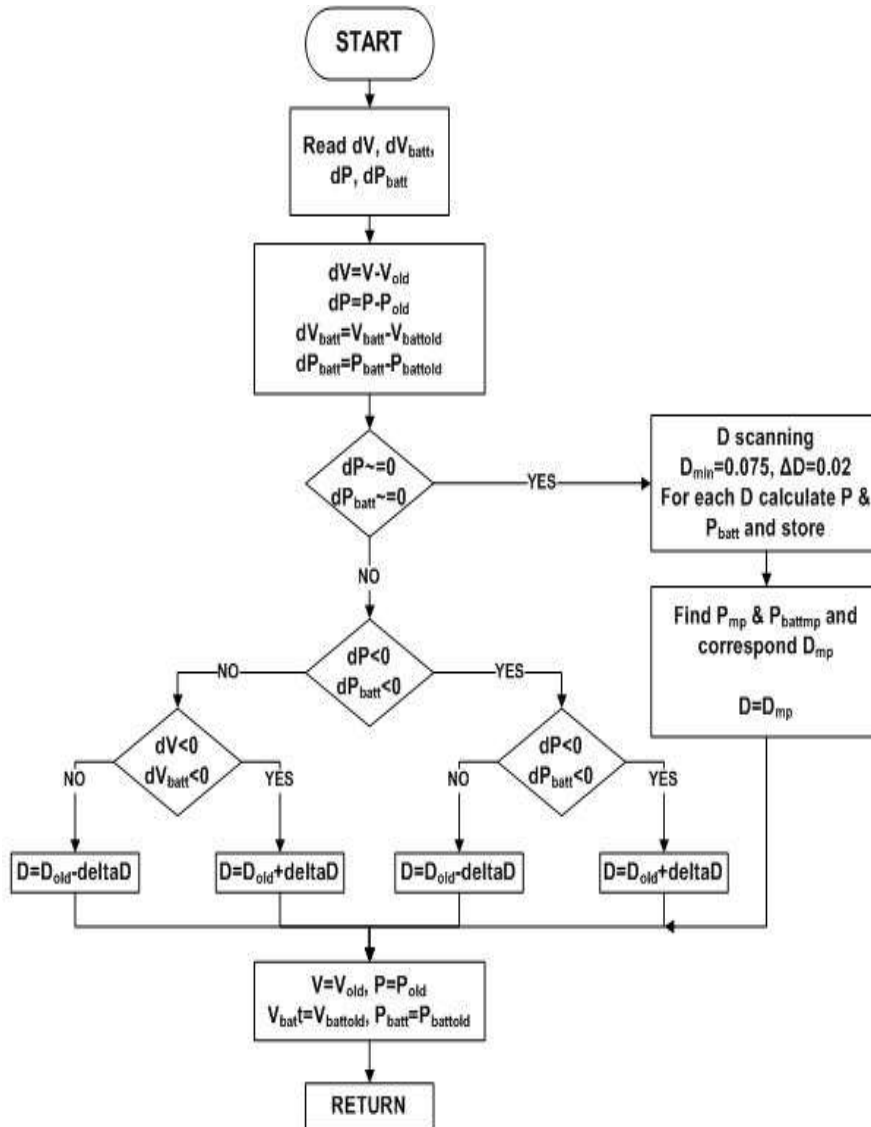
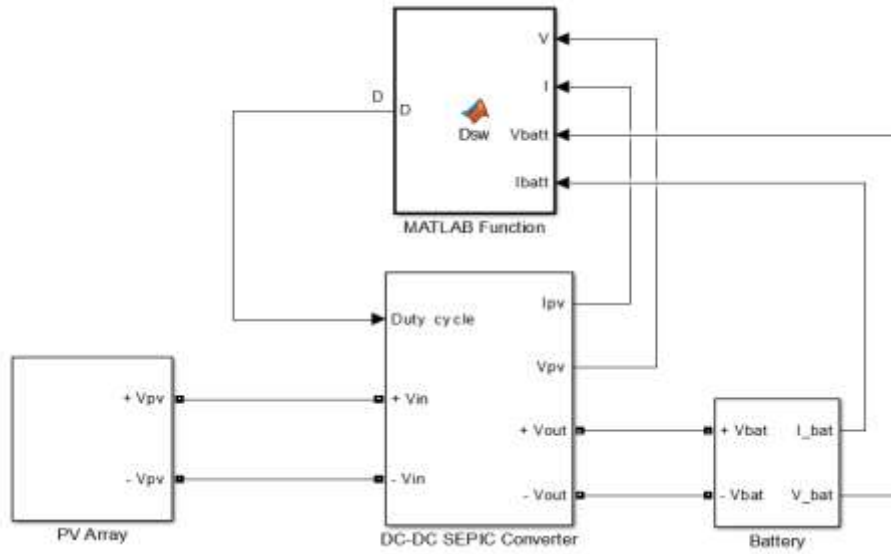


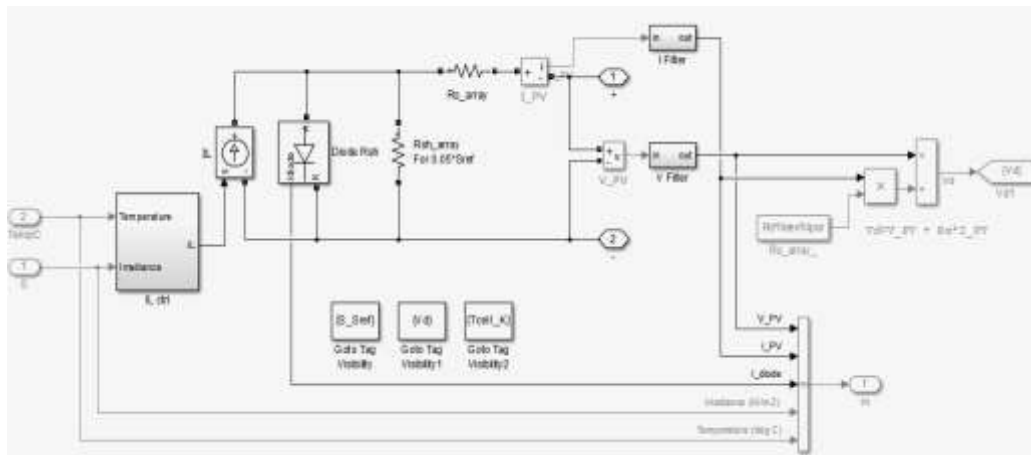
Figure 8. Flowchart of SEPIC converter duty cycle sweeping algorithm

### 3. Results and Analysis

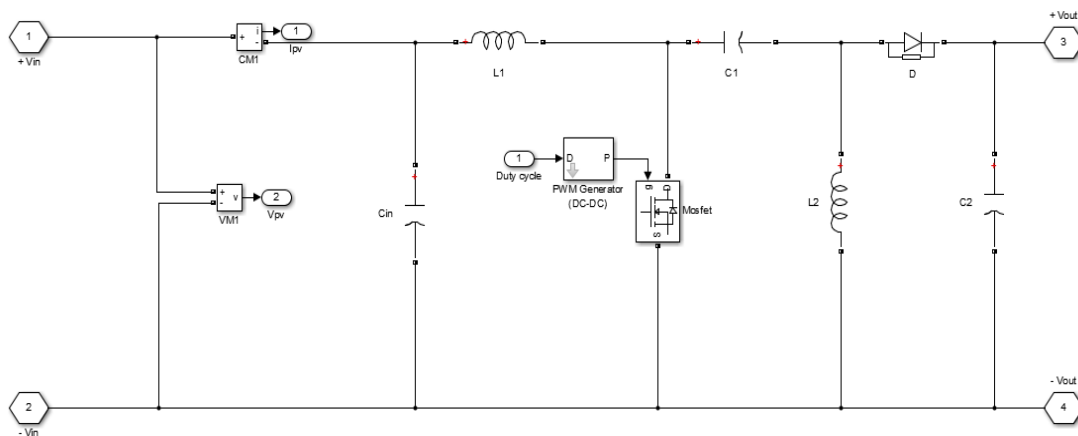
Figure 9 shows overall model of DC-DC SEPIC converter as maximum power point tracker and battery charger implemented in MATLAB/Simulink®. The output of the system is connected to 12V lead acid battery and the input of the system is connected to a PV array which is consist of 5 PV module connected in series. The specification of PV module used shows in Table 1. Typical values for 12V battery are as follow: overcharge voltage  $V_{oc}=15V$ , floating voltage  $V_{float}=13.5V$ , discharge threshold  $V_{chgenb}=10.5V$  and load disconnect voltage  $V_{idv}=11.4V$ . The switching frequency of the converter is chosen to be 200 kHz. For this simulation the duty cycle is set to be  $D_{min}=0.075$ ,  $D_{max}=0.875$  and  $\text{delta}D=0.05$ . Parameters for DC-DC SEPIC converter used in the simulation are as tabulated in Table 2.



(a) Overall simulation setup for SEPIC converter based MPPT charge controller

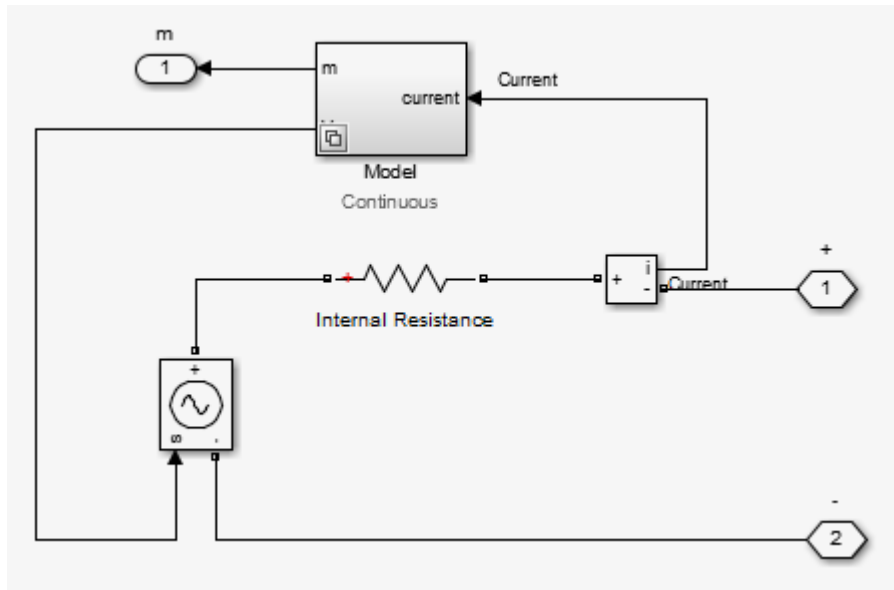


(b) Internal structure of the PV array



(c) Internal structure of the SEPIC converter

Figure 9(a-d). MATLAB/Simulink® model of SEPIC converter based MPPT charge controller



(d) Internal structure of the battery

Figure 9(a-d). MATLAB/Simulink® model of SEPIC converter based MPPT charge controller

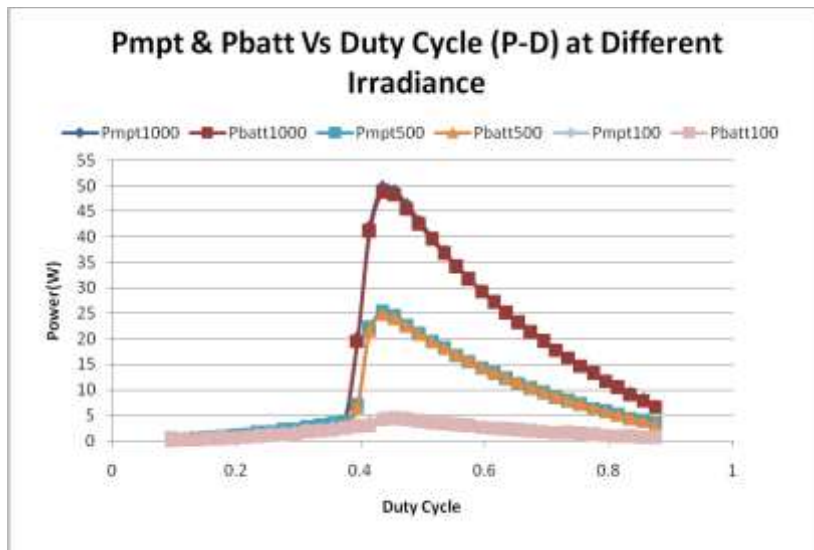


Figure 10. Comparison of SEPIC converter and battery output power

Table 3 (Appendix A) show the duty cycle ( $D$ ), maximum SEPIC converter output power ( $P_{mpt}$ ), battery power ( $P_{batt}$ ), maximum SEPIC converter voltage ( $V_{mp}$ ), maximum SEPIC converter current ( $I_{mp}$ ), battery voltage ( $V_{batt}$ ) and battery current ( $I_{batt}$ ) responses of the PV panel during the MPPT mode at irradiance of  $1000\text{W/m}^2$ ,  $500\text{W/m}^2$  and  $100\text{W/m}^2$  respectively. It can be seen in Figure 10 that the proposed duty cycle control algorithm is able to reach the MPP at duty cycle of 0.435 for the different irradiance  $1000\text{ W/m}^2$ ,  $500\text{ W/m}^2$  and  $100\text{ W/m}^2$ .

The simulation results of SEPIC converter for maximum power point tracking and standalone PV charging application under uniform irradiance conditions are shown in Figure 11 (Appendix B). For a solar irradiance of  $1000\text{ W/m}^2$ ,  $500\text{ W/m}^2$  and  $100\text{ W/m}^2$ , maximum power, battery voltage and current are shown in Figure 11(a), 11(b) and 11(c) respectively. During the

bulk charging phase (trickle and pre charging mode), the maximum available PV power is transferred to the battery stack, according to the MPPT algorithm. The charge regulation phase (CV mode) is initiated when the battery voltage rises to 13.21V (1000 W/m<sup>2</sup>)/13.15 (500 W/m<sup>2</sup>)/13.1 (100 W/m<sup>2</sup>) (Figure 11(a)/11(b)/11(c) second figure) and the battery charging current (Figure 11(a)/11(b)/11(c) third figure) is progressively reduced to 0.89A (1000 W/m<sup>2</sup>)/0.44A (500 W/m<sup>2</sup>)/ 0.08A (100 W/m<sup>2</sup>) at the end of this phase.

Table 3. Simulation results of implementing SEPIC converter as maximum power point tracking charge controller at different irradiance [Pmpt & Pbatt in Watt (W), Vmp & Vbatt in Volt (V), Imp & Ibatt in Ampere (A)]

Irr=500							Irr=1000						
D	Pmpt	Pbatt	Vmp	Imp	Vbatt	Ibatt	D	Pmpt	Pbatt	Vmp	Imp	Vbatt	Ibatt
0.295	2.336	1.739	21.667	0.108	13.095	0.133	0.295	2.464	1.841	22.308	0.111	13.096	0.141
0.315	2.615	1.994	21.651	0.121	13.096	0.152	0.315	2.795	2.145	22.295	0.125	13.096	0.164
0.335	2.951	2.309	21.632	0.136	13.097	0.176	0.335	3.112	2.443	22.283	0.140	13.097	0.187
0.355	3.271	2.615	21.615	0.151	13.098	0.200	0.355	3.467	2.784	22.269	0.156	13.098	0.213
0.375	3.627	2.964	21.594	0.168	13.099	0.226	0.375	3.859	3.169	22.254	0.173	13.099	0.242
0.395	7.163	6.541	21.383	0.335	13.105	0.499	0.395	20.135	19.541	21.567	0.934	13.126	1.489
0.415	22.118	21.628	19.905	1.111	13.130	1.647	0.415	41.918	41.097	20.185	2.077	13.164	3.122
0.435	25.228	24.823	18.421	1.370	13.139	1.889	0.435	49.738	48.750	18.772	2.650	13.183	3.698
0.455	24.326	24.034	17.015	1.430	13.143	1.829	0.455	49.185	48.280	17.381	2.830	13.191	3.660
0.475	22.723	22.523	15.718	1.446	13.145	1.714	0.475	46.267	45.517	16.076	2.878	13.195	3.450
0.495	21.094	20.973	14.522	1.453	13.146	1.595	0.495	43.051	42.451	14.867	2.896	13.199	3.216
0.515	19.554	19.517	13.418	1.457	13.148	1.485	0.515	39.961	39.507	13.750	2.906	13.201	2.993
0.535	18.116	18.150	12.397	1.461	13.149	1.380	0.535	37.063	36.731	12.717	2.915	13.204	2.782
0.555	16.773	16.850	11.450	1.465	13.150	1.281	0.555	34.352	34.108	11.757	2.922	13.206	2.583
0.575	15.514	15.626	10.567	1.468	13.151	1.188	0.575	31.812	31.640	10.863	2.929	13.208	2.396
0.595	14.334	14.489	9.743	1.471	13.151	1.102	0.595	29.430	29.330	10.028	2.935	13.209	2.221
0.615	13.229	13.423	8.974	1.474	13.152	1.021	0.615	27.197	27.155	9.249	2.941	13.210	2.056
0.635	12.189	12.401	8.254	1.477	13.153	0.943	0.635	25.097	25.085	8.519	2.946	13.211	1.899
0.655	11.208	11.418	7.576	1.479	13.153	0.868	0.655	23.113	23.110	7.832	2.951	13.212	1.749
0.675	10.279	10.489	6.937	1.482	13.153	0.797	0.675	21.236	21.240	7.184	2.956	13.213	1.608
0.695	9.400	9.624	6.335	1.484	13.154	0.732	0.695	19.461	19.478	6.574	2.960	13.213	1.474
0.715	8.572	8.812	5.768	1.486	13.154	0.670	0.715	17.786	17.810	6.000	2.965	13.214	1.348
0.735	7.791	8.032	5.236	1.488	13.154	0.611	0.735	16.205	16.212	5.459	2.969	13.214	1.227
0.755	7.050	7.268	4.732	1.490	13.154	0.553	0.755	14.705	14.668	4.947	2.972	13.213	1.110
0.775	6.342	6.516	4.251	1.492	13.153	0.495	0.775	13.270	13.173	4.459	2.976	13.213	0.997
0.795	5.658	5.793	3.789	1.493	13.153	0.440	0.795	11.888	11.739	3.990	2.980	13.213	0.889

Irr=100						
D	Pmpt	Pbatt	Vmp	Imp	Vbatt	Ibatt
0.295	1.995	1.469	19.951	0.100	13.095	0.112
0.315	2.214	1.667	19.891	0.111	13.095	0.127
0.335	2.462	1.899	19.818	0.124	13.096	0.145
0.355	2.734	2.158	19.729	0.139	13.097	0.165
0.375	2.995	2.414	19.636	0.153	13.097	0.184
0.395	3.274	2.695	19.524	0.168	13.098	0.206
0.415	3.597	3.027	19.372	0.186	13.099	0.231
0.435	4.762	4.259	18.118	0.263	13.102	0.325
0.455	4.751	4.315	16.715	0.284	13.103	0.329
0.475	4.463	4.096	15.428	0.289	13.103	0.313
0.495	4.146	3.828	14.244	0.291	13.104	0.292
0.515	3.841	3.551	13.152	0.292	13.104	0.271
0.535	3.556	3.295	12.140	0.293	13.104	0.251
0.555	3.289	3.072	11.201	0.294	13.105	0.234
0.575	3.039	2.873	10.328	0.294	13.105	0.219
0.595	2.806	2.677	9.515	0.295	13.105	0.204
0.615	2.587	2.476	8.755	0.295	13.105	0.189
0.635	2.380	2.271	8.041	0.296	13.105	0.173
0.655	2.185	2.079	7.370	0.297	13.105	0.159
0.675	2.001	1.910	6.737	0.297	13.105	0.146
0.695	1.826	1.768	6.141	0.297	13.105	0.135
0.715	1.662	1.642	5.582	0.298	13.105	0.125
0.735	1.508	1.518	5.056	0.298	13.105	0.116
0.755	1.361	1.381	4.560	0.299	13.105	0.105
0.775	1.222	1.226	4.087	0.299	13.105	0.094
0.795	1.087	1.068	3.631	0.299	13.105	0.082

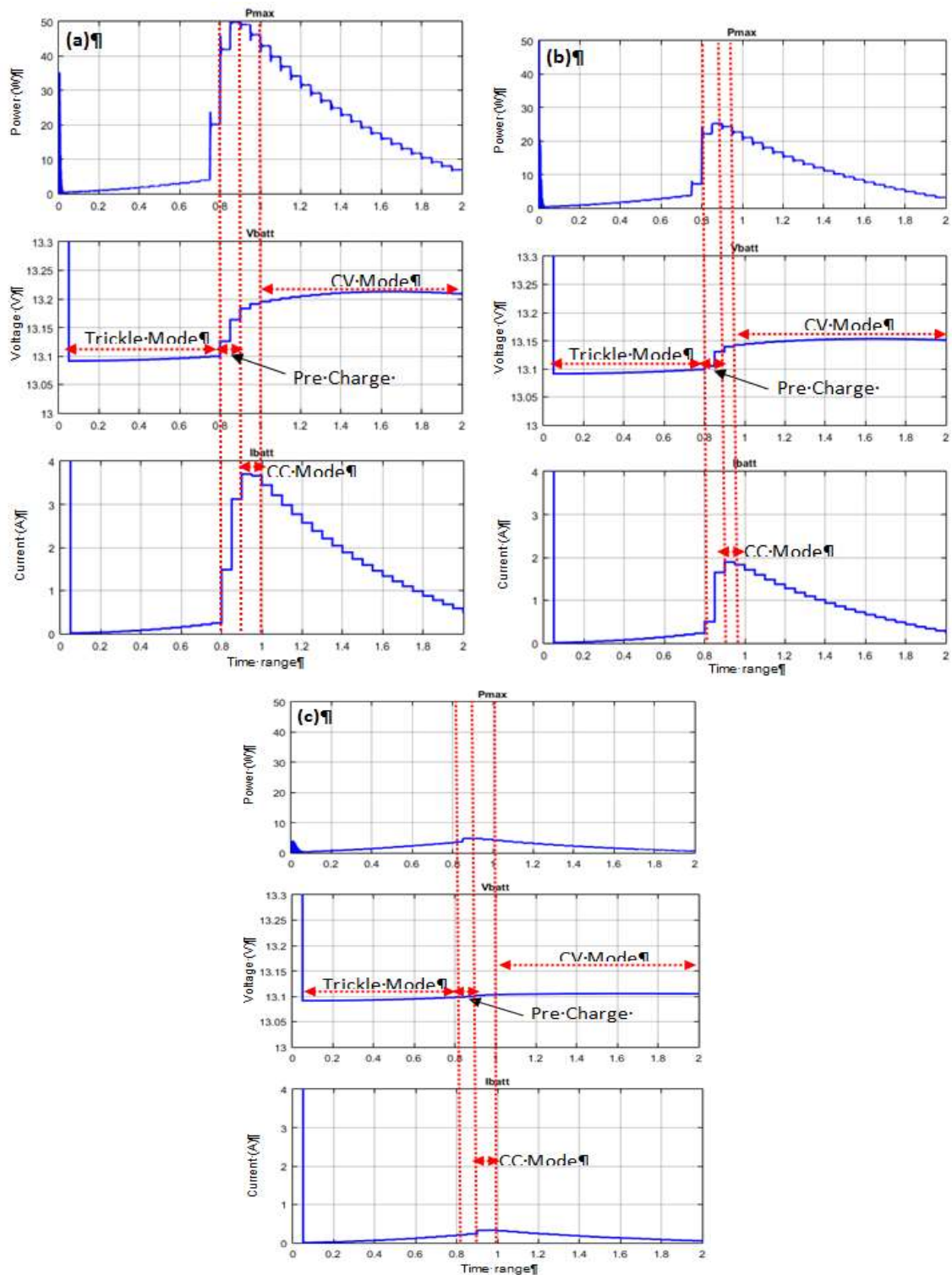


Figure 11. Battery voltage and current characteristic during MPPT

Overall, the system performs well under three different irradiance conditions, where it switches between maximum power point tracking and CV modes to maximize charging of the battery while maintaining the battery voltage within the allowable limit. During maximum power point tracking operation, the efficiency of SEPIC converter functioning as tracker is around

97.2-99.9% and the efficiency as solar charger is around 92.4-98.3%. The efficiency of SEPIC converter functioning as solar charger is lower compared to the maximum power point tracker within the range 1-5% based on Table 4 information. It is worth noting that the SEPIC converter efficiency drops during CV mode. This is due to the fact that the system is trying to maintain a constant charging voltage instead of operating at the maximum power point.

Table 4. Efficiency comparison of SEPIC converter for two different functions

PV array	Irradiance, G (W/m <sup>2</sup> )	Efficiency, $\eta$ (%)	
		MPP tracker	Battery charger
5 × 1 array (Series × Parallel)	1000	99.5	97.5
	500	99.9	98.3
	100	97.2	92.4

#### 4. Conclusion

In this paper, the development and analysis of SEPIC converter as MPPT charge controller for standalone PV system under uniform irradiance conditions is presented. The main aims are to extract maximum power from PV array and manage the power transfer to the storage system (battery) regardless of the changing in irradiation value. The efficiency of the proposed SEPIC converter is high which is 97.5% (as solar charger) and 99.5% (as maximum power tracker) at standard test condition. The result of this work leads to study, design and development of an intelligent energy management system, which optimizes the power transfer within a standalone PV system.

#### Acknowledgment

The authors would like to thank Universiti Malaysia Perlis and Ministry of Higher Education (MOHE) Malaysia for providing the facilities and financial support (Fundamental Research Grant Scheme (FRGS) under a grant number of FRGS/1/2015/TK10/UNIMAP/03/2.

#### References

- [1] P. Sharma and V. Agarwal. Exact maximum power point tracking of grid-connected partially shaded PV source using current compensation concept. *IEEE Trans. Power Electron.* 2014; 29(9): 4684–4692.
- [2] D. Sera, T. Kerekes, R. Teodorescu, and F. Blaabjerg. Improved MPPT Algorithms for Rapidly Changing Environmental Conditions. 2006; 1614–1619.
- [3] G. J. Kish, J. J. Lee, and P. W. Lehn. Modelling and control of photovoltaic panels utilising the incremental conductance method for maximum power point tracking. *IET Renew. Power Gener.* 2012; 6(4): 259.
- [4] N. Nnadi. Environmental / Climatic Effect on Stand-Alone Solar Energy Supply Performance for Sustainable Energy. *Niger. J. Technol.* 2012; 31(1): 79–88.
- [5] E. Kandemir, N. S. Cetin, and S. Borekci. A comprehensive overview of maximum power extraction methods for PV systems. 2017.
- [6] Y. E. Abu Eldahab, N. H. Saad, and A. Zekry. Enhancing the design of battery charging controllers for photovoltaic systems. *Renew. Sustain. Energy Rev.* 2016; 58: 646–655.
- [7] J. Yan, G. Xu, H. Qian, Y. Xu, and Z. Song. Model predictive control-based fast charging for vehicular batteries. *Energies.* 2011; 4(8): 1178–1196.
- [8] J. P. Dunlop. Batteries and Charge Control in Stand-Alone Photovoltaic Systems. *Sol. Energy.* 1997; 4(4): 265–270.
- [9] S. R. Osman, N. A. Rahim, J. Selvaraj, and Y. A. Al-Turki. Single sensor charging system with MPPT capability for standalone streetlight applications. *J. Power Electron.* 2015; 15(4): 929–938.
- [10] N. Asim, K. Sopian, S. Ahmadi, K. Saeedfar, M. A. Alghoul, O. Saadatian, and S. H. Zaidi. A review on the role of materials science in solar cells. *Renew. Sustain. Energy Rev.* 2012; 16(8): 5834–5847.
- [11] O. Bingöl and B. Özkaya. Analysis and comparison of different PV array configurations under partial shading conditions. *Sol. Energy.* 2018;160(July): 336–343.
- [12] A. Ingegnoli and A. Iannopolo. A Maximum power point tracking algorithm for stand-alone photovoltaic systems controlled by low computational power devices. *Appl. Power Electron. Colloq. (IAPEC), 2011 IEEE.* 2011; 22–27.
- [13] E. Karatepe, M. Boztepe, and M. Colak. Development of a suitable model for characterizing photovoltaic arrays with shaded solar cells. *Sol. Energy.* 2007; 81(8): 977–992.

- [14] M. G. Villalva, J. R. Gazoli, and E. R. Filho. Comprehensive approach to modeling and simulation of photovoltaic arrays. *IEEE Trans. Power Electron.* 2009;24(5):1198–1208.
- [15] K. Ishaque, Z. Salam, and Syafaruddin. A comprehensive MATLAB Simulink PV system simulator with partial shading capability based on two-diode model. *Sol. Energy.* 2011; 85(9): 2217–2227.
- [16] S. G. Tesfahunegn, P. J. S. Vie, Ulleberg, and T. M. Undeland. *A simplified battery charge controller for safety and increased utilization in standalone PV applications.* Conf. Rec. IEEE Photovolt. Spec. Conf.. 2011; 1: 002441–002447.
- [17] R.-J. Wai, W.-H. Wang, and C.-Y. Lin. High-Performance Stand-Alone Photovoltaic Generation System. *IEEE Trans. Ind. Electron.* 2008; 55(1): 240–250,.
- [18] C. Hua, J. Lin, and C. Shen. Implementation of a DSP-controlled PV system with peak power tracking. *IEEE Trans Ind Electron.* 1998; 45 (1):99–107.
- [19] N. Femia, G. Petrone, G. Spagnuolo, and M. Vitelli. Optimization of perturb and observe maximum power point tracking method. *IEEE Trans. Power Electron.* 2005;20(4):963–973.
- [20] M. A. Elgendy, B. Zahawi, and D. J. Atkinson. Assessment of Perturb and Observe MPPT Algorithm Implementation Techniques for PV Pumping Applications. *IET Conf. Publ.* 2012;; 592:P110.
- [21] O. Waszynczuk. Dynamic Behavior of a Class of Photovoltaic Power Systems. *IEEE Trans. Power Appar. Syst.* 1983; PAS-102(9):3031–3037.
- [22] B. Liu, S. Duan, F. Liu, and P. Xu. *Analysis and Improvement of Maximum Power Point Tracking Algorithm Based on Incremental Conductance Method for Photovoltaic Array.* 2007 7th Int. Conf. Power Electron. Drive Syst. 2007; 637–641,.
- [23] K. H. Hussein. Maximum photovoltaic power tracking: an algorithm for rapidly changing atmospheric conditions. *IEE Proc. - Gener. Transm. Distrib.* 1995; 142(1): 59.
- [24] Y. K. F. Liu, S. Duan, Fei Liu, B. Liu. A Variable Step Size INCMPPPT Method for PV Systems. *IEEE Trans. Ind. Electron.* 2008; 55(7):2622–2628.
- [25] A. Ait Laachir, A. El Kachani, A. Niaaniaa, M. B. Sedra, E. M. CHAKIR, and T. Jarou. Maximum Power Point Tracking Using Adaptive Fuzzy Logic control for Photovoltaic System. *Int. J. Eng. Res. Appl. (IJERA).* 2015; 5(1):65–70.
- [26] T. Senjyu and K. Uezato. *Maximum power point tracker using fuzzy control for photovoltaic arrays.* Proc. 1994 IEEE Int. Conf. Ind. Technol. - ICIT '94. 1994; (V);105–113.
- [27] Chung-Yuen Won, Duk-Heon Kim, Sei-Chan Kim, Won-Sam Kim, and Hack-Sung Kim. *A new maximum power point tracker of photovoltaic arrays using fuzzy controller.* Proc. 1994 Power Electron. Spec. Conf. - PESC'94. 1994; 396–403.
- [28] M. Unlu, S. Camur, and B. Arifoglu. A new maximum power point tracking method for PV systems under partially shaded conditions. *Int. Conf. Power Eng. Energy Electr. Drives.* 2013; 1346–1351.